

Discovery of H₂O maser emission from the red supergiant IRAS04553–6825 in the Large Magellanic Cloud

Jacco Th. van Loon¹, Peter te Lintel Hekker², Valentín Bujarrabal³, Albert A. Zijlstra⁴, and Lars-Åke Nyman^{5,6}

¹ Astronomical Institute “Anton Pannekoek”, University of Amsterdam, Kruislaan 403, 1098 SJ Amsterdam, The Netherlands

² Australia Telescope National Facility, Parkes Observatory, P.O.Box 276, Parkes, NSW 2870, Australia

³ Observatorio Astronómico Nacional, Campus Universitario, Apartado 1143, E-28800 Alcalá de Henares (Madrid), Spain

⁴ University of Manchester Institute of Science and Technology, P.O.Box 88, Manchester M60 1QD, UK

⁵ European Southern Observatory, Casilla 19001, Santiago 19, Chile

⁶ Onsala Space Observatory, S-439 92 Onsala, Sweden

Received 21 April 1998 / Accepted 25 May 1998

Abstract. We report the detection of 22 GHz H₂O maser emission from the red supergiant IRAS04553–6825 in the Large Magellanic Cloud. It is the first known source of circumstellar H₂O maser emission outside the Milky Way. The measured flux density is comparable to that expected from scaling the galactic red supergiant NML Cyg. The peak velocity agrees with the SiO maser peak velocity.

A near-infrared spectrum indicates that IRAS04553–6825 has a typical LMC metallicity. We argue that, possibly as a result of the low metallicity, the H₂O emission probably occurs near or within the dust formation radius, rather than further out as appears to be the case in NML Cyg and galactic OH/IR stars.

Key words: masers – circumstellar matter – stars: late-type – stars: mass-loss – supergiants – Magellanic Clouds

1. Introduction

Maser emission from evolved stars is associated with dusty, oxygen rich circumstellar envelopes (CSEs), mainly around red supergiants (RSGs) and stars at the tip of the Asymptotic Giant Branch (AGB) (Elitzur 1992; Habing 1996). The strongest maser lines originate from OH (at 1612 MHz), H₂O (at 22 GHz), and SiO (at 43 and 86 GHz), located progressively deeper into the CSE. Hence these lines are used to trace the mass-loss history and velocity structure of the CSE, through their photon fluxes and line profiles (Chapman & Cohen 1986; Lewis 1989, 1990). Maser lines are also excellent tracers of the stellar space velocity and have been used to map the kinematics and mass distribution in our Galaxy (e.g. Lindqvist et al. 1992; Sevenster et al. 1995).

Circumstellar OH and SiO maser emission has recently been detected in the Large Magellanic Cloud (LMC) (Wood et al. 1986, 1992; van Loon et al. 1996, 1998a). Wood et al. (1992) argue that the outflow velocities in CSEs of OH/IR stars in the LMC are a factor two lower than in corresponding Milky Way stars, a difference they attribute to less efficient driving of the

outflow caused by the lower metallicity in the LMC. However, Zijlstra et al. (1996) find the difference to be only 20 to 30%, from their analysis of the same data. Moreover, the SiO maser emission from the LMC RSG IRAS04553–6825 (van Loon et al. 1996) showed that in this case, the outflow velocity as derived from the OH maser profile was underestimated by more than a factor two. The relation between outflow velocity and metallicity is therefore still uncertain.

In the LMC, SiO maser emission is generally too faint to be detected, with IRAS04553–6825 the only successful detection to date. Stellar H₂O maser emission has not been found outside the Galaxy before.

Here we present the discovery of the first extra-galactic source of circumstellar H₂O maser emission — viz. the RSG IRAS04553–6825 in the LMC. We also present spectroscopic results that confirm the LMC metallicity of its stellar photosphere. We then discuss the implications for the structure of the CSE by comparing with the galactic red supergiant NML Cyg.

2. Observations and results

2.1. H₂O radio observations

The observations were performed on August 19, 20 of 1997, using the 64 m radio telescope at Parkes, Australia. We observed the $6_{16} \rightarrow 5_{23}$ rotational transition of ortho-H₂O at a rest frequency of 22.235 GHz, using the 1.3 cm receiver plus autocorrelator backend. The 64 MHz band width and 1024 channels centred at ~ 22.21 GHz yield a velocity coverage of ~ 860 km s⁻¹ at 0.84 km s⁻¹ channel⁻¹. Using the Dual Circular feed we simultaneously obtained spectra in left and right circular polarization. The beam FWHM is 1.4', the system temperature is typically 110 K, and the conversion factor from antenna temperature to flux density is 6.3 Jy K⁻¹. The nearby sky was measured every two minutes, resulting in very flat baselines that required only a very shallow second-order polynomial to be subtracted.

We observed the LMC RSG IRAS04553–6825 for six hours on-source integration. No difference was found between the

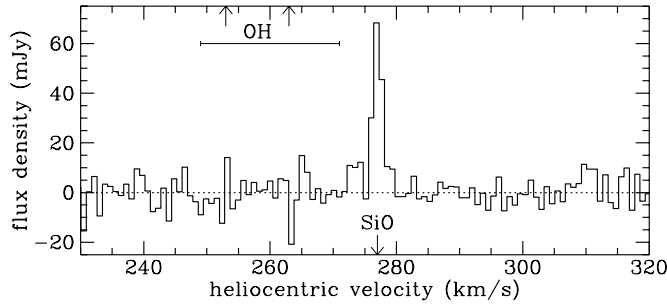


Fig. 1. Discovery spectrum of the 22 GHz H₂O maser emission from LMC red supergiant IRAS04553–6825. The velocities are heliocentric. Also indicated are the peak velocities of the 86 GHz SiO and 1612 MHz OH masers (arrows) and the total velocity extent of the 1612 MHz OH maser (bar)

spectra obtained at either polarization, which we then averaged. The final 22-GHz spectrum of IRAS04553–6825 is presented in Fig. 1, with flux densities in mJy and heliocentric velocities in km s⁻¹. The measured rms (1 σ) is only 5.5 mJy.

We detected a single peak of H₂O maser emission with a peak flux density of 68 mJy (with 20% calibration accuracy), corresponding to a 12 σ detection. The peak is centred at a heliocentric velocity of 277 km s⁻¹, and has a FWHM of 1.7 km s⁻¹. The integrated flux of the emission is 0.17 Jy km s⁻¹.

2.2. CaII triplet echelle spectroscopy

We used the 3.5 m New Technology Telescope (NTT) at the European Southern Observatory (ESO) at La Silla, Chile, on January 7, 1996, with the ESO Multi-Mode Instrument (EMMI), to obtain an echelle spectrum of IRAS04553–6825. Grating #14 and grism #4 as cross disperser were used, yielding a spectral coverage of 6000–9000 Å. The slit width and length were 2'' and 4'', respectively. The integration time was one hour.

The data were reduced in the normal way using the Munich Interactive Data Analysis Software (MIDAS) package. The wavelength calibration was done by taking a ThAr lamp spectrum in conditions identical to the spectrum of IRAS04553–6825. The measured spectral resolving power is $\sim 4 \times 10^4$.

The equivalent width of the Ca II triplet lines at 8498, 8542, and 8662 Å measures the surface gravity in giants and supergiants, if the metallicity is known. Reversely, if an estimate of the surface gravity is available from knowledge of spectral type and luminosity, the Ca II lines can be used to infer the metallicity.

The echelle spectrum of IRAS04553–6825 around the Ca II triplet is presented in Fig. 2, on an arbitrary flux scale. The equivalent widths of the two strongest components are measured as $W_{8542} = 1.6 \pm 0.1$ Å and $W_{8662} = 1.7 \pm 0.1$ Å. Their sum is $W_{8542+8662} = 3.3 \pm 0.2$ Å.

The Ca II absorption is maximum at a heliocentric velocity of ~ 300 km s⁻¹, corresponding to a redshift with respect to the stellar velocity of a little less than the outflow velocity in the outer parts of the CSE. This is explained by scattering

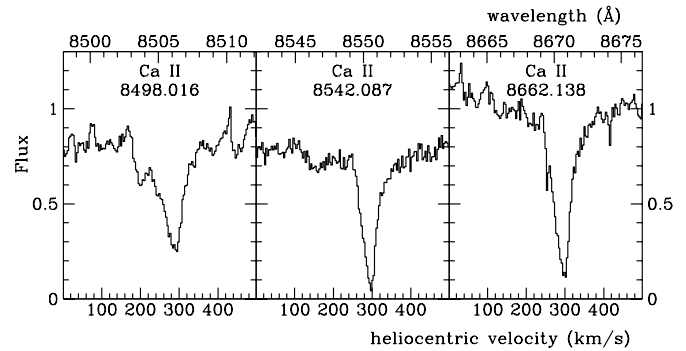


Fig. 2. Echelle spectra of the Ca II triplet lines in IRAS04553–6825

of the photospheric spectrum by an extended, expanding dust shell. The measured equivalent widths of the Ca II lines are not affected by the scattering (see Romanik & Leung 1981, and references therein).

For IRAS04553–6825 we adopt a bolometric luminosity of $L \sim 4 \times 10^5 L_{\odot}$, and an effective temperature between 2500 and 3000 K (spectral type: M7 supergiant). The surface gravity must then be about $\log g \sim 0$ cm s⁻². If we then compare the measured equivalent width of the Ca II triplet with the results from García-Vargas et al. (1998), we find that consistency is only achieved if the metallicity of IRAS04553–6825 is a factor two to three lower than solar. This result is not very sensitive to the values of the adopted stellar parameters, and hence we conclude that IRAS04553–6825 has a typical LMC metallicity ($Z = 0.008$).

3. Discussion

3.1. Circumstellar H₂O masers in the LMC

The detection of IRAS04553–6825 shows that H₂O masers in the LMC with photon fluxes of 10^{44} s⁻¹ are detected at a 5 σ level within 6 hours of on-source integration, with the current receiver at Parkes. Typical observed H₂O maser photon fluxes from galactic sources are between 10^{43} s⁻¹ (Lindqvist et al. 1990) and 10^{44-45} s⁻¹ (Nyman et al. 1986) for OH/IR stars, 10^{41-44} s⁻¹ for irregular and semiregular red variables with mass-loss rates $\sim 10^{-7} M_{\odot}$ yr⁻¹ (Szymczak & Engels 1997), 10^{43-44} s⁻¹ for Mira variables (Benson & Little-Marenin 1996; Yates et al. 1995), and 10^{44-45} s⁻¹ for supergiants (Yates et al. 1995). This implies that many of the mass-losing RSGs and AGB stars (i.e. IRAS point sources) in the LMC are expected to have detectable H₂O maser emission.

3.2. Introduction to IRAS04553–6825

With a bolometric luminosity $M_{\text{bol}} = -9.3$ mag and a spectral type M7, IRAS04553–6825 was recognised to be the most luminous (very) red supergiant in the LMC by Elias et al. (1986). The progenitor mass was estimated $M_{\text{ZAMS}} \sim 50 M_{\odot}$ by Zijlstra et al. (1996). The current mass-loss rate of $\dot{M} \sim \text{few } 10^{-4} M_{\odot}$ yr⁻¹ was estimated from the self-absorbed 10 μm silicate

dust feature by Roche et al. (1993), who argue that the lower than expected extinction in the optical indicates a diskly CSE.

IRAS04553–6825 exhibits strong OH 1612 MHz and weaker 1665 MHz mainline emission (Wood et al. 1986, 1992). Comparison of the SiO maser peak velocity and the OH maser emission profile revealed that OH is only observed from the blue-shifted part of the shell. The outflow velocity is 27 km s⁻¹, similar to Milky Way RSGs. (Wood et al. derived 10 km s⁻¹ as is suggested by the OH maser emission profile alone.) It is possible that the red-shifted emission is much weaker than the blue-shifted and therefore below the detection limit. Stronger blue-shifted emission is expected if the maser amplifies emission from within the shell. Alternatively, an asymmetric and structured OH profile can also arise from bipolar outflow (Chapman 1988; te Lintel Hekkert et al. 1988).

3.3. Similarities between IRAS04553–6825 and NML Cyg

IRAS04553–6825 is remarkably similar to NML Cyg, a well known RSG in the Milky Way (Johnson 1967; Diamond et al. 1984; Richards et al. 1996; Monnier et al. 1997), in terms of luminosity, progenitor mass, spectral type, pulsation period, mass-loss rate, 10 μm feature profile, outflow velocity, CSE geometry, OH maser emission profile and peak flux density (scaled to a common distance of 1 kpc), and SiO maser photon flux. The properties of the two stars are compared in Table 1. We compiled the infrared photometry from the data provided in Gezari et al. (1993), and use $F_{8\mu m}(\text{zeromag}) = 2 \times 10^{-12} \text{ W m}^{-2} \mu\text{m}^{-1} = 42.7 \text{ Jy}$. The H₂O properties (NML Cyg: Yates et al. 1995) are also included in Table 1.

The pump efficiency of SiO masers is known to be related to the pulsation amplitude (Alcolea et al. 1990): Mira variables and semi-regular variables with visual amplitudes exceeding 2.5 mag always reach the maximum efficiency, while variables with smaller amplitudes are usually less efficient. We recalculated the pump efficiency of the SiO masers $F_{\text{SiO}}/F_{8\mu m}$. The pumping in IRAS04553–6825 is twice as efficient as in NML Cyg, but a factor ~ 4 less than in Mira variables. The SiO maser emission of IRAS04553–6825 has a larger ratio $F_{\text{int}}/F_{\text{max}}$ than NML Cyg (at a common resolution of 0.7 km s⁻¹), and a few times as large as Mira variables (Alcolea et al. 1990; van Loon et al. 1996).

The near-infrared (JHKL) amplitudes are 0.4 mag for NML Cyg (Gezari et al. 1993) and 0.3 mag for IRAS04553–6825 (Wood et al. 1992). For NML Cyg, Kholopov et al. (1985) list a magnitude range of 11.19 to 12.54 mag in R, and 17.0 to 18.0 mag in V. We have sparse optical photometry of IRAS04553–6825 in the period 1994–1997, suggesting an amplitude in V of ~ 2 mag (smaller in R). We conclude that the pulsation properties of NML Cyg and IRAS04553–6825 are similar, with possibly IRAS04553–6825 closer resembling Mira variables.

From the similar properties of both objects we predicted to detect 22 GHz H₂O maser emission from IRAS04553–6825 at a level of ~ 60 mJy (van Loon 1998b). The measured peak flux density is in excellent agreement with this prediction.

Table 1. Comparison between the properties of the red supergiants NML Cyg in the Milky Way and IRAS04553–6825 in the LMC.

	NML Cyg	IRAS04553–6825
Bolo. Luminosity	$5 \times 10^5 L_{\odot}$	$4 \times 10^5 L_{\odot}$
Distance	2 kpc	50 kpc
Progenitor Mass	$\sim 50 M_{\odot}$	$\sim 50 M_{\odot}$
Spectral Type	M6	M7
Pulsation Period	940 days	930 days
Mass-loss Rate	$1.8 \times 10^{-4} M_{\odot} \text{ yr}^{-1}$	$\sim 5 \times 10^{-4} M_{\odot} \text{ yr}^{-1}$
10 μm Silicate	emission+absorption	emission+absorption
(K – L) colour	2.4 mag	1.9 mag
(H – K) colour	2.0 mag	1.2 mag
Outflow Velocity	28 km s ⁻¹	27 km s ⁻¹
CSE Geometry	disk + bipolar	disk + bipolar
OH Profile	blue asymm./duplicit	blue asymm./duplicit
OH Peak (1 kpc)	1.1 kJy	1.0 kJy
OH Photon Flux	$4 \times 10^{45} \text{ s}^{-1}$	$3.7 \times 10^{45} \text{ s}^{-1}$
SiO Profile	peak + broad comp.	peak + broad comp.
SiO Peak (1 kpc)	144 Jy	270 Jy
SiO Photon Flux	$0.6 \times 10^{45} \text{ s}^{-1}$	$2.6 \times 10^{45} \text{ s}^{-1}$
$F_{\text{SiO}}/F_{8\mu m}$	$\frac{1}{90}$	$\frac{1}{43}$
$F_{\text{int}}/F_{\text{max}}(\text{SiO})$	7.3 km s ⁻¹	15.7 km s ⁻¹
H ₂ O Profile	blue-shifted maximum	stellar velocity
H ₂ O Peak (1 kpc)	160 Jy	170 Jy
H ₂ O Photon Flux	$2.6 \times 10^{44} \text{ s}^{-1}$	$2.6 \times 10^{44} \text{ s}^{-1}$

3.4. Location of the H₂O masers

A striking difference between the H₂O masers of IRAS04553–6825 and NML Cyg is that in IRAS04553–6825 the emission peaks at the stellar restframe velocity, whereas in NML Cyg the line profile resembles the OH maser line profile.

Interferometric observations of the masers around NML Cyg indicate that its H₂O masers are amplified radially and that they are located in the dusty part of the CSE, where radiation pressure on the grains accelerates the outflowing matter (Richards et al. 1996). Indeed, in NML Cyg the strongest emission occurs at a blueshift of ~ 20 km s⁻¹.

The peak of H₂O maser emission from IRAS04553–6825 falls within ~ 1 km s⁻¹ of the stellar velocity (as inferred from the SiO velocity), and all emission is detected within a range of 8 km s⁻¹. This is similar to the situation in Mira variables, indicating low outflow velocities in the H₂O masing region of the CSE (Yates et al. 1995). In contrast, NML Cyg is similar to the OH/IR stars.

Cooke & Elitzur (1985) derive a scaling relation for estimating the inner radius r_q of the H₂O masing region, below which the density is higher than $\sim 10^9 \text{ cm}^{-3}$ and the maser is quenched. This was confirmed by observations (Yates & Cohen 1994). The collision rate is dominated by collisions with H₂ and does therefore not depend on metallicity: we therefore expect that the same relation will hold in the LMC. With an outflow velocity at r_q of 0.8 km s⁻¹ (half the FWHM of the H₂O maser peak), and an average particle mass of $2 \times 10^{-24} \text{ g}$, we estimate $r_q \sim 4 \times 10^{15} \text{ cm}$, or ~ 20 times the stellar radius. This is outside the region where the SiO maser occurs (Humphreys et al. 1996).

We speculate that in IRAS04553–6825 the H₂O maser originates near the dust formation radius, where the logarithmic velocity gradient is very high ($d(\ln(v))/d(\ln(r)) \gtrsim 1$) and tangential amplification dominates over radial amplification. Part of the emission may also originate from inside the dust formation radius where outflow velocities are low. Both cases could explain the narrow H₂O peak coinciding with the tangentially amplified SiO maser peak (see also Engels et al. 1997). The H₂O masers in NML Cyg are located outside of the dust formation region, where the outflow velocities are already $\gtrsim 15 \text{ km s}^{-1}$ (Richards et al. 1996).

In this model, either the maser occurs closer to the star in IRAS04553–6825, or dust formation takes place further out (as in galactic Miras as compared to galactic OH/IR stars). The first possibility appears less likely if the inner radius is set by collisional quenching of the population inversion. It would be interesting to test whether at lower metallicity the dust formation and the acceleration of the outflow occurs at larger radii because of the relative lack of refractory elements: in this case the difference between NML Cyg and IRAS04553–6825 could be a generic difference between similar stars in the Milky Way and the LMC.

Acknowledgements. We would like to thank Drs. Marcus Price and Ian Stewart for help with the observations at Parkes. We also thank Dr. Roland Gredel for help with the NTT observations at La Silla, that were performed in Director’s Discretionary Time. We thank Dr. Anita Richards for helpful discussions, and an anonymous referee for her/his remarks that helped improve the paper. This research was partly supported by the NWO under Pionier Grant 600-78-333. O jacco agradece ao anjinho Joana por ser para ele como ele queria ser para ela.

References

- Alcolea J., Bujarrabal V., Gómez-González J., 1990, A&A 231, 431
 Benson P.J., Little-Marenin I.R., 1996, ApJS 106, 579
 Chapman J.M., Cohen R.J., 1986, MNRAS 220, 513
 Chapman J.M., 1988, MNRAS 230, 415
 Cooke B., Elitzur M., 1985, ApJ 295, 175
 Diamond P.J., Norris R.P., Booth R.S., 1984, MNRAS 207, 611
 Elias J.H., Frogel J.A., Schwering P.B.W., 1986, ApJ 302, 675
 Elitzur M., 1992, ARA&A 30, 75
 Engels D., Winnberg A., Walmsley C.M., Brand J., 1997, A&A 322, 291
 García-Vargas M.L., Mollá M., Bressan A., 1998, A&A in press
 Gezari D.Y., Schmitz M., Pitts P.S., Mead J.M., 1993, “Catalog of Infrared Observations”, 3rd Edition, NASA Reference Publication 1294
 Habing H.J., 1996, A&AR 7, 97
 Humphreys E.M.L., Gray M.D., Yates J.A., et al., 1996, MNRAS 282, 1359
 Johnson H.L., 1967, ApJ 149, 345
 Kholopov P.N., Samus’ N.N., Frolov M.S., et al., 1985, “General Catalogue of Variable Stars”, 4th Edition, Vol. II, Nauka Publishing House, Moscow
 Lewis B.M., 1989, ApJ 338, 234
 Lewis B.M., 1990, AJ 99, 710
 Lindqvist M., Winnberg A., Forster J.R., 1990, A&A 229, 165
 Lindqvist M., Habing H.J., Winnberg A., 1992, A&A 259, 118

- Monnier J.D., Bester M., Danchi W.C., et al., 1997, ApJ 481, 420
 Nyman L.-Å., Johansson L.E.B., Booth R.S., 1986, A&A 160, 352
 Richards A.M.S., Yates J.A., Cohen R.J., 1996, MNRAS 282, 665
 Roche P.F., Aitken D.K., Smith C.H., 1993, MNRAS 262, 301
 Romanik C.J., Leung C.M., 1981, ApJ 246, 935
 Sevenster M.N., DeJonghe H., Habing H.J., 1995, A&A 299, 689
 Szymczak M., Engels D., 1997, A&A 322, 159
 te Lintel Hekkert P., Habing H.J., Caswell J.L., Norris R.P., Haynes R.F., 1988, A&A 202, L19
 van Loon J.Th., Zijlstra A.A., Bujarrabal V., Nyman L.-Å., 1996, A&A 306, L29
 van Loon J.Th., Zijlstra A.A., Whitelock P.A., Loup C., te Lintel Hekkert P., et al., 1998a, A&A 329, 169
 van Loon J.Th., 1998b, in: “ISO’s View on Stellar Evolution”, eds. L.B.F.M. Waters, C. Waelkens, K.A. van der Hucht and P.A. Zaal, Kluwer Academic Publishers, p405
 Wood P.R., Bessell M.S., Whiteoak J.B., 1986, ApJ 306, L81
 Wood P.R., Whiteoak J.B., Hughes S.M.G., et al., 1992, ApJ 397, 552
 Yates J.A., Cohen R.J., 1994, MNRAS 270, 958
 Yates J.A., Cohen R.J., Hills R.E., 1995, MNRAS 273, 529
 Zijlstra A.A., Loup C., Waters L.B.F.M., et al., 1996, MNRAS 279, 32